IET Renewable Power Generation

Research Article

IET Journals
The Institution of Engineering and Technology

Convex probabilistic allocation of wind generation in smart distribution networks

ISSN 1752-1416
Received on 13th February 2017
Revised 13th May 2017
Accepted on 29th May 2017
E-First on 20th June 2017
doi: 10.1049/iet-rpg.2017.0100
www.ietdl.org

Mohammad-Amin Akbari[1], Jamshid Aghaei[1] ✉, Mostafa Barani[1]

[1]*Department of Electrical and Electronic Engineering, Shiraz University of Technology, Shiraz, Iran*

✉ *E-mail: aghaei@sutech.ac.ir*

Abstract: This study introduces a probabilistic optimisation model for allocation of renewable distributed generations (DGs) in radial distribution networks. The methodology is based on a probabilistic generation – load model that combines all possible operating conditions of the wind-based DG units as well as load levels with their probabilities. A multiobjective performance index is extracted that is formulated as a combination of two indices, namely energy losses reduction and voltage improvement. Besides, a probabilistic AC optimal power flow is used to determine the optimal allocation of wind DG and maximise the multiobjective performance index. Two alternative control approaches of the future smart grids, i.e. area based under load tap changer control and adaptive power factor control, are assessed to maximise potential benefits and expand the penetration level of DGs. At first, this problem is formulated as a mixed-integer non-linear programming (MINLP) which leads to a computationally NP-hard problem. Accordingly, the obtained MINLP problem is relaxed and reformulated in the form of a well-suited second-order cone programming problem which is computationally efficient scheme to be solved. The implementation of the proposed framework on 4-bus and IEEE 33-bus radial distribution systems shows the performance of the proposed optimisation mechanism.

1 Introduction

As a result of economic and environmental advantages as well as governmental incentives, there has been paid increasing attention in the usage of renewable energies. At the end of 2015, renewable energies provided 23.7% of the worldwide energy production [1]. Among all types of renewable energy resources, the share of the wind power is 3.7% (433 GW) as reported in [2]. The integration of wind power in the power system affects distribution system (DS) operation and planning practices of distribution network operators and distribution companies from both technical and economic implications points of view [3–7].

The optimal distributed generation placement (ODGP) problem seeks to find optimal sites and sizes of distributed generation (DG) units to be installed in the distribution networks subject to the technical, DG operation, and investment constraints. The ODGP is known as a complicated mixed-integer non-linear programming (MINLP) optimisation problem. From the literature, the methods of solving ODGP problem can be classified into analytical [8, 5, 6, 9–12], numerical [13–17], and population-based [18–23] methods. The main disadvantage of the traditionally analytical approach is that only one static scenario is considered to calculate the impact of indices of DGs, while the DG output power and demand have time-varying nature. Several works attempt to overcome this issue [5, 6]. Distributed time-varying generation through a multiobjective index has been introduced in [5] for evaluating DGs impacts on DSs. New probabilistic-based performance indices have been defined in [6]. Drawback of these analytical methods is that for a considered time period, only specified penetration of DGs can be assessed and this means that an iterative procedure is required for multiple connections of DGs. Thus, these methods result in only declarative solutions.

As mentioned, ODGP problem belongs to the MINLP problems which are well known for their complexity and computationally expensive features. Due to the lack of efficient mathematical approaches for solving this class of optimisation problems within a reasonable time, heuristic algorithms have been widely used in the literature to find fast suboptimal solutions. Such methods despite their broad applicabilities (e.g. for black-box models) often neglect the intrinsic structure of problems which is important for large-scale problems. To cope with this end, the obtained non-linear programming problem is relaxed and reformulated as a well-studied second-order cone programming problem (SOCP) [24] which is efficient in terms of computational burden.

Existing operational rules and policies are based on the passive operation of the distribution network. This passive operation which is based on the minimum consumption and the maximum production can restrict the capacity of the connected renewable energy resources [13]. In contrast, an active distribution network will affect the potential benefits of DGs [25, 26]. Two alternative control approaches are assessed to maximise the potential benefits as well as the penetration level of DGs, i.e. area-based under load tap changer (ULTC) coordinated voltage control (CVC) and adaptive power factor control (PFc). The latter is the approach that has been pursued in Spain [3], where renewable and combined heat and power DG units contribute to the growing amount of the available reactive power for using during peak hours and consume reactive power during off peak hours. There is a growing demand for the development of the distribution network from a passive network to an active one with the purpose of facilitating cumulative levels of the embedded generation. At this point, a recent procedure is advanced to determine the appropriate sites and sizes of wind generation (WG) in distribution networks considering practical constraints as well as to maximise the benefits of renewable energy generations.

Overall, few studies in ODGP have properly investigated the potential benefits of CVC and PFc for maximising the technical benefits of DG in radial DS (RDS) considering the stochastic nature of load and renewable generation. In addition, providing a convex formulation of optimal power flow (OPF) has been largely neglected. Our approach is to formulate ODGP by optimal adjustment of ULTC and power factor of WGs as a stochastic-convex OPF problem.

2 Uncertainty characterisation

This section explains the probabilistic modelling of the load, WG and complete generation-load model.

Table 1 Calculated load states, ND = 10

d	PD_d	pd_d	d	PD_d	pd_d
1	1.0000	0.0100	6	0.5850	0.1630
2	0.8530	0.0560	7	0.5100	0.1630
3	0.7740	0.1057	8	0.4510	0.0912
4	0.7130	0.1654	9	0.4060	0.0473
5	0.6500	0.1654	10	0.3510	0.0330

Table 2 Wind power states, NW = 12

w	PG_w	pw_w	w	PG_w	pw_w
1	1.0000	0.0784	7	0.4499	0.0912
2	0.9497	0.0250	8	0.3499	0.1122
3	0.8497	0.0326	9	0.1999	0.1037
4	0.7498	0.0451	10	0.1500	0.1123
5	0.6498	0.0501	11	0.0500	0.0661
6	0.5498	0.0773	12	0.0000	0.2059

2.1 Probabilistic modelling of loads

For the sake of accurate decision making, planners can use many tools to forecast future peak loads. Assuming the system peak load follows the IEEE-RTS system [27], implementing a clustering technique and utilising the central centroid sorting process developed in [28], we can split the load into ND segments with different probabilities. The dth segment has a probability of pd_d and an average value of D_d. Table 1 shows the calculated load states supplemented by their probabilities.

2.2 Probabilistic modelling of WG

Hourly output generation for each WG, during a whole year, has been modelled according to the historical data and specific WG technology characteristics. The hourly wind speed data for the site under study have been utilised to generate a Rayleigh PDF [29] for each time period

$$f_v = \left(\frac{2v}{c^2}\right)\exp\left[-\left(\frac{v}{c}\right)^2\right] \tag{1}$$

Here, c is called the scale factor which is equal to $1.128v_m$; v_m is the mean value of the wind speed for a site considered. The continuous PDF is sliced into NW strips of equal widths. Area of the wth strip gives the probability pw_w of the wind speed with a mean value of W_w. WGs real output power corresponding to each state can be calculated using mean values of wind speeds and wind turbine power curve parameters (see Table 2)

$$PG_w = \begin{cases} 0, & v_{ci} \le W_w \le v_r \\ P_{rated} \times \dfrac{(W_w - v_{ci})}{(v_r - v_{ci})}, & 0 \le W_w \le v_{ci} \\ P_{rated}, & v_r \le W_w \le v_{co} \\ 0, & v_{co} \le W_w \end{cases} \tag{2}$$

where v_{ci}, v_r and v_{co} are the cut-in speed, rated speed and cutoff speed of the wind turbine, respectively. Hence, in this paper, WG is modelled as a probabilistic negative real power load with an equivalent set of NW pair values of Rayleigh probability density function (PDF). PFc can be accomplished by optimally setting of power factors that should be kept by WGs at each time period. PFc strategy encourages WGs, e.g. doubly-fed induction generators, to inject reactive power during peak periods and absorb reactive power during off peak periods. The reactive power is assumed to be a decision variable which should be determined by the optimisation problem. A typical wind turbine with the rated power of 1.1 MW, the cut-in speed of 4 m/s, the rated speed of 14 m/s, and the cut-out speed of 24 m/s is considered in this paper. The annual capacity factor of the wind turbine is found to be 0.22.

2.3 Complete probabilistic generation-load model

From the aforementioned modelling of WGs output power and system load, the complete generation-load model can be obtained. As mentioned, the system loads can be modelled as ND states of loads with their corresponding probabilities. Besides, WGs can be modelled as NW states with generation values and their probabilities. Considering all possible combinations, $ND \times NW$ probable states will be obtained. Each probable state $s = 1, 2, \ldots, ND \times NW$ has the probability of $pd_d \times pw_w$, the WG output power of PG_w and the load of D_d (see Table 3). The corresponding probabilities of the generation-load states are shown in Table 4.

3 Problem formulation

3.1 Notations

An RDS can be represented by the graph $H(\mathcal{N}, \mathcal{E})$, the set of substations $\mathcal{N}^F \subseteq \mathcal{N}$ and the set of generator buses $\mathcal{N}^G \subseteq \mathcal{N}$. Let $\mathcal{N} := \{1, \ldots, NB\}$ denotes the collection of all nodes. Each line connects an ordered pair (i, j) of nodes where node i is the sending end and node j is the receiving end bus. Let $\mathcal{E}$ denotes the collection of all lines, and $(i, j) \in \mathcal{E}$ is abbreviated by $i \to j$ for convenience. Note that, as H is directed, if $(i, j) \in \mathcal{E}$ then $(j, i) \notin \mathcal{E}$. Let s denotes the index of generation-load states, where $s \in \mathcal{S}$ in which $\mathcal{S}$ is the set of all possible generation-load states with the $ND \times NW$ elements. For each bus $i \in \mathcal{N}$, let $V_{is} = V_{is}^{re} + \boldsymbol{i}V_{is}^{im}$ denotes the complex voltage. Specifically, the substation voltages are equipped with ULTC. Let $SD_{is} = PD_{is} + \boldsymbol{i}QD_{is}$ defines the given apparent power of the load connected to bus $i \in \mathcal{N}$ (zero whenever bus i is not connected to any load) and $SW_{is} = PW_{is} + \boldsymbol{i}QW_{is}$ defines the apparent power of the WGs connected to bus $i \in \mathcal{N}^G$ at state s. Note that, PW_{is} can be calculated as the product of nominal installed capacity of WGs at bus i, W_i, and PG_s. For each line $(i, j) \in \mathcal{E}$, let $z_{ij} = r_{ij} + \boldsymbol{i}x_{ij}$ denotes its impedance. Let $I_{ijs} = I_{ijs}^{re} + \boldsymbol{i}I_{ijs}^{im}$ denotes the complex current from buses i to j. Let $S_{ijs} = P_{ijs} + \boldsymbol{i}Q_{ijs}$ denotes the sending-end power flow from buses i to j where P_{ijs} and Q_{ijs} denote the real and reactive power flow, respectively.

3.2 Constraints

The following constraints are assumed in the proposed stochastic-non-convex OPF model.

3.2.1 Power flow equations: Given the network graph $(\mathcal{N}, \mathcal{E})$, the decision variables satisfy the *DistFlow* equations [30]. For each line $(i, j)/(j, h) \in \mathcal{E}$ and state $s \in \mathcal{S}$,

Table 3 Complete generation-load states, $s \in \mathcal{S} = \{1, 2, \ldots, 120\}$

s	PG_s	PD_s	s	PG_s	PD_s	s	PG_s	PD_s	s	PG_s	PD_s
1	1.0000	1.0000	31	0.7497	1.0000	61	0.4498	1.0000	91	0.1499	1.0000
2	1.0000	0.8530	32	0.7497	0.8530	62	0.4498	0.8530	92	0.1499	0.8530
3	1.0000	0.7740	33	0.7497	0.7740	63	0.4498	0.7740	93	0.1499	0.7740
4	1.0000	0.7130	34	0.7497	0.7130	64	0.4498	0.7130	94	0.1499	0.7130
5	1.0000	0.6500	35	0.7497	0.6500	65	0.4498	0.6500	95	0.1499	0.6500
6	1.0000	0.5850	36	0.7497	0.5850	66	0.4498	0.5850	96	0.1499	0.5850
7	1.0000	0.5100	37	0.7497	0.5100	67	0.4498	0.5100	97	0.1499	0.5100
8	1.0000	0.4510	38	0.7497	0.4510	68	0.4498	0.4510	98	0.1499	0.4510
9	1.0000	0.4060	39	0.7497	0.4060	69	0.4498	0.4060	99	0.1499	0.4060
10	1.0000	0.3510	40	0.7497	0.3510	70	0.4498	0.3510	100	0.1499	0.3510
11	0.9497	1.0000	41	0.7497	1.0000	71	0.3498	1.0000	101	0.0499	1.0000
12	0.9497	0.8530	42	0.7497	0.8530	72	0.3498	0.8530	102	0.0499	0.8530
13	0.9497	0.7740	43	0.7497	0.7740	73	0.3498	0.7740	103	0.0499	0.7740
14	0.9497	0.7130	44	0.7497	0.7130	74	0.3498	0.7130	104	0.0499	0.7130
15	0.9497	0.6500	45	0.7497	0.6500	75	0.3498	0.6500	105	0.0499	0.6500
16	0.9497	0.5850	46	0.7497	0.5850	76	0.3498	0.5850	106	0.0499	0.5850
17	0.9497	0.5100	47	0.7497	0.5100	77	0.3498	0.5100	107	0.0499	0.5100
18	0.9497	0.4510	48	0.7497	0.4510	78	0.3498	0.4510	108	0.0499	0.4510
19	0.9497	0.4060	49	0.7497	0.4060	79	0.3498	0.4060	109	0.0499	0.4060
20	0.9497	0.3510	50	0.7497	0.3510	80	0.3498	0.3510	110	0.0499	0.3510
21	0.8497	1.0000	51	0.7497	1.0000	81	0.1999	1.0000	111	0.0000	1.0000
22	0.8497	0.8530	52	0.7497	0.8530	82	0.1999	0.8530	112	0.0000	0.8530
23	0.8497	0.7740	53	0.7497	0.7740	83	0.1999	0.7740	113	0.0000	0.7740
24	0.8497	0.7130	54	0.7497	0.7130	84	0.1999	0.7130	114	0.0000	0.7130
25	0.8497	0.6500	55	0.7497	0.6500	85	0.1999	0.6500	115	0.0000	0.6500
26	0.8497	0.5850	56	0.7497	0.5850	86	0.1999	0.5850	116	0.0000	0.5850
27	0.8497	0.5100	57	0.7497	0.5100	87	0.1999	0.5100	117	0.0000	0.5100
28	0.8497	0.4510	58	0.7497	0.4510	88	0.1999	0.4510	118	0.0000	0.4510
29	0.8497	0.4060	59	0.7497	0.4060	89	0.1999	0.4060	119	0.0000	0.4060
30	0.8497	0.3510	60	0.7497	0.3510	90	0.1999	0.3510	120	0.0000	0.3510

$$P_{ijs} - r_{ij}\left|I_{ijs}\right|^2 = -\mathrm{PW}_{js} + \mathrm{PD}_{js} + \sum_{h:\, j \to h} P_{jhs} \tag{3}$$

$$Q_{ijs} - x_{ij}\left|I_{ijs}\right|^2 = -\mathrm{QW}_{js} + \mathrm{QD}_{js} + \sum_{h:\, j \to h} Q_{jhs} \tag{4}$$

$$|V_{is}|^2 - \left|V_{js}\right|^2 = 2\left(r_{ij}P_{ijs} + x_{ij}Q_{ijs}\right) - \left|z_{ij}\right|^2\left|I_{ijs}\right|^2 \tag{5}$$

3.2.2 Branch current equation: The line current through $(i, j) \in \mathscr{E}$ can be expressed as follows:

$$\left|I_{ijs}\right|^2 = \frac{P_{ijs}^2 + Q_{ijs}^2}{\left|V_{is}\right|^2}, \quad \forall (i, j) \in \mathscr{E},\ \forall s \in \mathcal{S} \tag{6}$$

3.2.3 Voltage limits: Voltage magnitudes should lie within pre-specified voltage lower bound, V_i^-, and upper bound, V_i^+:

$$V_i^- \le |V_{is}| \le V_i^+, \quad \forall i \in \mathcal{N}/\mathcal{N}^F,\ \forall s \in \mathcal{S} \tag{7}$$

3.2.4 Line thermal limits: Thermal limits of the substations and lines are generally assumed to be stiff and no overloading is permitted. The current flowing through the lines is limited by their maximum thermal capacity as follows I_{ij}^+:

$$\left|I_{ijs}\right| \le I_{ij}^+, \quad \forall (i, j) \in \mathscr{E},\ \forall s \in \mathcal{S} \tag{8}$$

3.2.5 Adaptive power factor control for WGs: WGs can operate at a range of power factors. It is expected that WGs be capable of adopting a scheme in which the power factor of each generator is dispatched for each period within a given range. The operating power factor of WGs may need to be regulated by considering corresponding standards

$$\mathrm{pf}^- \le \frac{\mathrm{PW}_{is}}{\sqrt{\mathrm{PW}_{is}^2 + \mathrm{QW}_{is}^2}} \le 1, \quad \forall i \in \mathcal{N}^G,\ \forall s \in \mathcal{S} \tag{9}$$

where pf^- is the specified lower limit of the operating power factor of a WGs site.

3.2.6 Optimal ULTC adjustment: By implementing ULTC, more WGs may be installed in the system. As ULTC can be changed dynamically at the substation, voltage profile and line losses may be changed, too. The ULTC model follows standard OPF practice in allowing the best tap setting to be chosen [31]. The voltage magnitude at the substation buses is considered as a decision variable that should satisfy the following constraints:

$$V_i^- \le |V_{is}| \le V_i^+, \quad \forall i \in \mathcal{N}^F,\ \forall s \in \mathcal{S} \tag{10}$$

3.3 Objective functions

Depending on the system states such as site, size and power factor of WGs, the ULTC tap position and load demand, technical attributes such as losses and voltage profile can be improved if these variables optimally determined, and vice versa. By introducing WGs in the system, line losses can be reduced and voltage profile can be improved because WGs can provide a portion of the real and reactive power to the load, thus helping to decrease the current along a section of the distribution line, which, in turn, will result in a reduction of line losses and boost in the voltage magnitude at the customer site [8].

Table 4 Probabilities of calculated generation-load states, $s \in \mathcal{S} = \{1, 2, \ldots, 120\}$

s	ρ_s	s	ρ_s	s	ρ_s	s	ρ_s
1	0.0008	31	0.0005	61	0.0009	91	0.0011
2	0.0043	32	0.0026	62	0.0053	92	0.0065
3	0.0083	33	0.0050	63	0.0101	93	0.0125
4	0.0126	34	0.0076	64	0.0153	94	0.0188
5	0.0126	35	0.0076	65	0.0153	95	0.0188
6	0.0124	36	0.0074	66	0.0151	96	0.0185
7	0.0126	37	0.0076	67	0.0153	97	0.0188
8	0.0069	38	0.0042	68	0.0084	98	0.0104
9	0.0036	39	0.0022	69	0.0044	99	0.0054
10	0.0027	40	0.0016	70	0.0033	100	0.0040
11	0.0003	41	0.0005	71	0.0011	101	0.0006
12	0.0014	42	0.0028	72	0.0065	102	0.0037
13	0.0028	43	0.0053	73	0.0125	103	0.0071
14	0.0042	44	0.0080	74	0.0188	104	0.0107
15	0.0042	45	0.0080	75	0.0188	105	0.0107
16	0.0041	46	0.0079	76	0.0185	106	0.0106
17	0.0042	47	0.0080	77	0.0188	107	0.0107
18	0.0023	48	0.0044	78	0.0104	108	0.0059
19	0.0012	49	0.0023	79	0.0054	109	0.0031
20	0.0009	50	0.0017	80	0.0040	110	0.0023
21	0.0003	51	0.0008	81	0.0011	111	0.0020
22	0.0019	52	0.0045	82	0.0060	112	0.0116
23	0.0036	53	0.0086	83	0.0115	113	0.0224
24	0.0055	54	0.0129	84	0.0174	114	0.0337
25	0.0055	55	0.0129	85	0.0174	115	0.0337
26	0.0054	56	0.0128	86	0.0171	116	0.0332
27	0.0055	57	0.0130	87	0.0174	117	0.0337
28	0.0030	58	0.0071	88	0.0096	118	0.0186
29	0.0016	59	0.0037	89	0.0050	119	0.0096
30	0.0012	60	0.0028	90	0.0037	120	0.0072

3.3.1 Energy losses reduction index: Line energy losses are considered to be minimised over a time horizon which briefly are defined below. Active energy losses, EL^{re}, and reactive energy losses, EL^{im}, related to the real and imaginary parts of line apparent losses can be expressed by

$$EL^{re} = \sum_{(i,j) \in \mathscr{E}} \sum_{s \in \mathcal{S}} \rho_s r_{ij} |I_{ijs}|^2 T \tag{11}$$

$$EL^{im} = \sum_{(i,j) \in \mathscr{E}} \sum_{s \in \mathcal{S}} \rho_s x_{ij} |I_{ijs}|^2 T \tag{12}$$

Here, ρ_s is the probability of state s and T is the duration of planning time horizon which in this paper is assumed to be 8760 h. A proper integration of WGs would reduce total energy losses which are defined as the following index:

$$LI = \frac{EL^{re} + EL^{im}}{EL^{0}} \tag{13}$$

Here, EL^0 is the energy loss without WGs addition, i.e. base case system.

3.3.2 Voltage improvement index: The improvement of the voltage profile in the presence of WGs is quantified by the voltage improvement index, VI. Mathematically, it is defined as follows:

$$VI = \sum_{i \in \mathcal{N}} \sum_{s \in \mathcal{S}} \rho_s k_i \left(\frac{|V_{is}|}{|V_{i0}|} \right)^2 \tag{14}$$

Here, $|V_{i0}|$ is the magnitude of complex voltage at bus i before WGs addition. k_i is the importance factor of load buses which can be chosen based on the importance and criticality of the loads [8]. For the sake of simplicity, all the load busses are equally weighted in this paper, i.e. $k_i = 1/\mathrm{NB}$, $\forall i$, where NB is the total number of load buses in the system.

3.3.3 Multiobjective index: When WGs are allocated for energy losses minimisation, the penetration level may be limited to have maximum voltage profile, and vice versa. To include the effects of the aforementioned indices in the ODGP problem, the following multiobjective index, MOI, can be used as the objective function which should be maximised

$$MOI = -\beta_1 LI + \beta_2 VI \tag{15}$$

Here, the weighting factors $0 \leq (\beta_1, \beta_2) \leq 1$, which $\beta_1 + \beta_2 = 1$, indicate the relative importance of each index for allocation of WGs. The choice of these factors mainly depends on the experiments and concerns of planners or decision makers. Equal weights are assumed for the proposed indices in this paper.

Generally, the highest value of VI implies the most beneficial allocation of WGs in terms of the voltage profile maximisation. Also, the lowest value of LI implies the highest benefit in terms of energy losses minimisation. Furthermore, the highest MOI implies the maximum benefit of WGs integration in terms of energy losses reduction and voltage profile improvement.

3.4 Overall problem definition

The proposed stochastic-non-convex OPF problem seeks to maximise the benefit of WGs by optimal allocation and operation of WGs subject to the power flow equations (3)–(5), branch current equation (6), voltage limits (7), thermal limits (8), power factor regulation of WG site (9) and ULTC adjustment constraint (10).

The following optimisation problem summarises the OPF formulation for the radial networks, where the power flows are expressed in the *Distflow* model:

$$\text{OPF:} \max_{x \in \mathscr{X}} \text{MOI} \tag{16}$$

$$\text{s.t.} \quad (3)-(15) \tag{17}$$

Over

$$\mathscr{X} := (P, Q, \text{PW}, \text{QW}, |V|, |I|) \tag{18}$$

where $\mathscr{X}$ is the set of decision vectors.

It is clear that the objective function (16) is convex over $\mathscr{X}$. While the feasible set $\mathscr{X}^*$ that satisfies (3)–(10), makes the problem to be non-convex belonging to the NP-hard problems.

3.5 Stochastic-convex formulation of OPF problem

Equality constraint in (6) is the source of non-convexity. It can be relaxed by the inequality (19) over all lines to obtain the SOCP relaxation of the proposed OPF problem:

$$\left|I_{ijs}\right|^2 \geq \frac{P_{ijs}^2 + Q_{ijs}^2}{\left|V_{is}\right|^2}, \quad \forall (i,j) \in \mathscr{E} \tag{19}$$

Now, we define new variables to represent the voltage and line current magnitudes

$$\upsilon_{is} := \left|V_{is}\right|^2, \quad \forall i \in \mathscr{N}^{\text{G}}, \forall s \in \mathscr{S} \tag{20}$$

$$l_{ijs} := \left|I_{ijs}\right|^2, \quad \forall (i,j) \in \mathscr{E}, \forall s \in \mathscr{S} \tag{21}$$

$$\text{SW}_{is} := \sqrt{\text{PW}_{is}^2 + \text{QW}_{is}^2}, \quad \forall i \in \mathscr{N}^{\text{G}}, \forall s \in \mathscr{S} \tag{22}$$

Thus, the stochastic-convex OPF model for WGs integration can be summarised as follows:

$$\text{SOCP:} \max_{y \in \mathscr{Y}} \text{MOI} \tag{23}$$

$$\text{s.t.} \quad \text{LI} = \frac{\text{EL}^{\text{re}} + \text{EL}^{\text{im}}}{\text{EL}^{0}} \tag{24}$$

$$\text{VI} = \sum_{i \in \mathscr{N}} \sum_{s \in \mathscr{S}} \rho_s k_i \frac{\upsilon_{is}}{\left|V_{i0}\right|^2} \tag{25}$$

$$\text{EL}^{\text{re}} = \sum_{(i,j) \in \mathscr{E}} \sum_{s \in \mathscr{S}} \rho_s r_{ij} \left|l_{ijs}\right|^2 T \tag{26}$$

$$\text{EL}^{\text{im}} = \sum_{(i,j) \in \mathscr{E}} \sum_{s \in \mathscr{S}} \rho_s x_{ij} \left|l_{ijs}\right|^2 T \tag{27}$$

$\forall (i,j)/(j,h) \in \mathscr{E}$ and $\forall s \in \mathscr{S}$:

$$P_{ijs} - r_{ij} l_{ijs} = -\text{PW}_{js} + \text{PD}_{js} + \sum_{h:\, j \to h} P_{jhs} \tag{28}$$

$$Q_{ijs} - x_{ij} l_{ijs} = -\text{QW}_{js} + \text{QD}_{js} + \sum_{h:\, j \to h} Q_{jhs} \tag{29}$$

$$\upsilon_{is} - \upsilon_{js} = 2\left(r_{ij} P_{ijs} + x_{ij} Q_{ijs}\right) - \left|z_{ij}\right|^2 l_{ijs} \tag{30}$$

$$l_{ijs} \geq \frac{P_{ijs}^2 + Q_{ijs}^2}{\upsilon_{is}} \tag{31}$$

$$l_{ijs} \leq I_{ij}^{+2} \tag{32}$$

$$l_{ijs} \geq 0 \tag{33}$$

$\forall i \in \mathscr{N}$ and $\forall s \in \mathscr{S}$:

$$V_i^{-2} \leq \upsilon_{is} \leq V_i^{+2} \tag{34}$$

$$\upsilon_{is} \geq 0 \tag{35}$$

$\forall i \in \mathscr{N}^{\text{G}}$ and $\forall s \in \mathscr{S}$:

$$\text{pf}^{-} \leq \frac{\text{PW}_{is}}{\text{SW}_{is}} \leq 1 \tag{36}$$

$$\text{SW}_{is} \geq \sqrt{\text{PW}_{is}^2 + \text{QW}_{is}^2}, \quad \forall i \in \mathscr{N}^{\text{G}}, \forall s \in \mathscr{S} \tag{37}$$

$$\text{SW}_{is} \geq 0, \quad \forall i \in \mathscr{N}^{\text{G}}, \forall s \in \mathscr{S} \tag{38}$$

Over

$$\mathscr{Y} := (P, Q, \text{PW}, \text{QW}, \text{SW}, \upsilon, l) \tag{39}$$

If the solution to SOCP (23)–(39) is feasible for the OPF (16)–(18), i.e. it satisfies (6), then it is a global optimum of the OPF (16)–(18), in which case we say that the SOCP relaxation is exact.

4 Case study

In this section, two test systems are used to illustrate the effectiveness of the proposed optimisation framework. Each single objective problem has been solved using the modelling language GAMS [32] and solver MOSEK on a computer with Pentium(R) Dual-Core CPU @ 2 GHz and 4 GB of RAM. Note that the resulting non-linear conic constraints result in 'linear' constraints in general algebraic modeling system (GAMS). Thus, the original non-linear formulation is in fact, a linear model in GAMS.

4.1 Snapshot versus stochastic generation-load model

Neglecting the uncertainties of load and wind speed in the ODGP problem leads to 'suboptimal' solutions. For the sake of simplicity, the impact of WGs on the proposed performance indices is investigated on a simple 4-bus test feeder. The network peak load is 7.5 MW. The voltage at the grid supply point (GSP), i.e. secondary busbar, is set at 1.01 pu. The line between buses 1 and 2 (considering the two parallel transformers) has the reactance of 0.125 pu and maximum thermal limit of 0.6 pu on 100-MVA base. These parameters are similar for lines 2–3 and 3–4 i.e. $r_{23} = r_{34} = 0.196$ pu, $x_{23} = x_{34} = 0.1427$ pu and $I_{23}^{+} = I_{34}^{+} = 0.155$ pu.

Three cases are assumed here:

Case 1: A snapshot generation-load model (peak load demand and constant wind power generation scenario).
Case 2: A constant generation and probabilistic load model (as presented in Table 1).
Case 3: A stochastic generation-load model based on the data given in Tables 3 and 4.

The effects of WG increasing penetration level on the LI, VI and MOI metrics can be seen in Fig. 1. The results indicate that the deterministic analysis, i.e. case 1, depending on the WG capacity leads to over/under estimating solutions. The largest capacity with the most benefit can be obtained by case 1. When the most realistic case, i.e. case 3, is considered, the benefits are less significant while at the most of the times, the actual power injection is lower than the nominal capacity.

Also, this figure indicates that due to considering the variability and stochastic nature of WG and load, case 3 permits more capacity to be installed.

4.2 Optimal placement and smart operation of WG units

The proposed problem of optimal placement and smart operation of WGs has been applied to the IEEE 33-bus radial test DS. This system has a peak demand of 3.715 MW and 2.300 MVAr [30].

While in annual energy terms, the aggregated demand profile implies an annual consumption of 670.5 MWh and 446.7 MVArh.

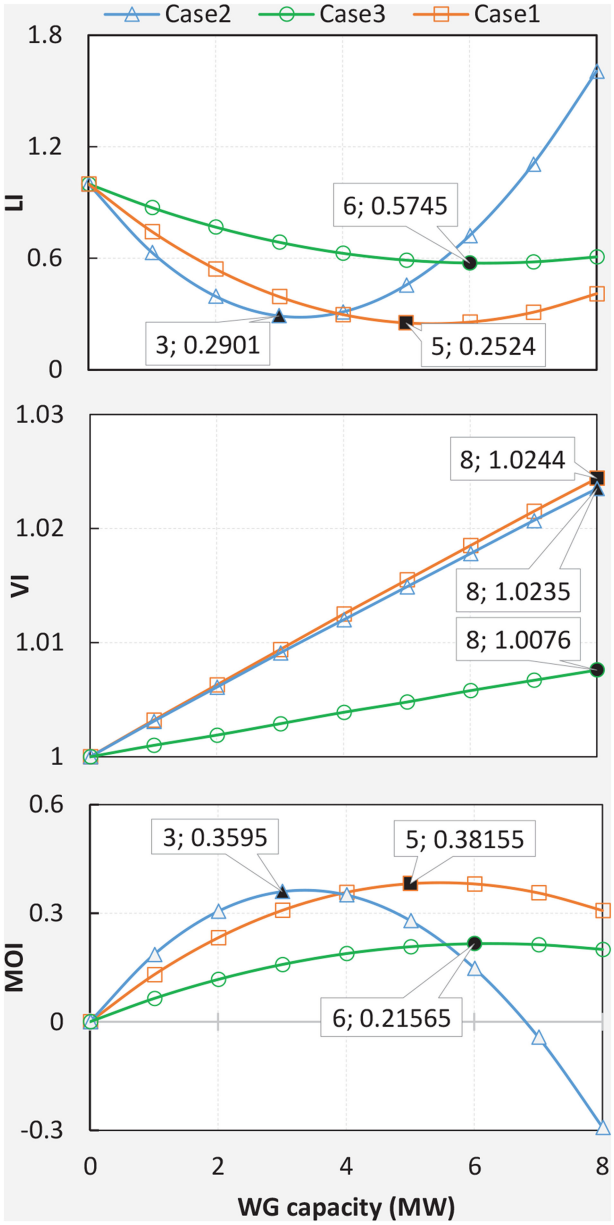

Fig. 1 *Effects of WG increasing penetration on the LI, VI and MOI indices obtained by cases 1–3*

Base values of this system are 12.66 kV and 100 MVA. The substation voltage magnitude is assumed at nominal value in the base case (no DG). The constraint of operating voltages is assumed to be ±5% of nominal value. The ULTC target voltage is assumed to be 1.05. Single-line diagram of this system can be seen in Fig. 2. Detailed load and branch data of this test system are obtained from [30]. This radial test system was modified to evaluate the effects of DG penetration. Eight candidate buses of WGs (WG1–WG8) are assumed to be installed in the system [33, 31], as shown in Fig. 2. The maximum thermal limits of lines are set to 6.6 MVA (which corresponds to a current of 300 A).

The effects of passive and active operations of network are evaluated and discussed here. Note that, the uncertainties of the both load and generation are considered in the OPF problem. For the obtained probabilistic model of generation and load, and for a given candidate location of WGs, stochastic-convex OPF problem is performed over a horizon of 1 year for the business as usual (BAU) operation of system and two control schemes. Optimal size and location of WGs are recorded for these operation scenarios. The results are then compared and discussed.

Table 5 presents the optimum values of MOI, LI, VI and maximum installation capacity of WG under various operating strategies and without exceeding voltage or thermal limits. Take a brief look, it can be observed that MOI in the active operation of network will be greater than those when passive operation is adopted. However, compared to the base case (without WG), considerable benefits are achieved by optimal allocation of WGs in the system. Unity power factor operation of the WGs in the case of BAU is obtained MOI of 0.2061. If CVC scheme is incorporated, then this benefit is increased by >17%. From all the case studies, the assumption of both CVC and PFc gives the highest benefit with the MOI of 0.3449. In this case, the energy losses are reduced by 65% and voltage profile is improved by 13.82%. It should be mentioned that a fast and reliable communication system must be installed throughout the entire system, interacting with WG units in order to enable the centralised control of the entire system [4]. In these control strategies, the cost effectiveness of using further control mechanisms is questionable.

The last row of Table 5 shows the total capacity of the installed WGs in the system for different operating scenarios. In comparison to BAU operation of the system, by only 1.6% increment in WG capacity when WGs are assumed to operate at 0.98 lead power factor, the CVC scheme permits 16% increment in MOI. The explanation is that, implementation of CVC strategy has diminished voltage rise issues in most states.

PFc strategy allows WGs to inject reactive power during peak periods and absorb reactive power during off peak periods. In the case of PFc scheme without CVC it can be observed that, in comparison with the CVC with unity and 0.98 lag power factors, much more benefit can be achieved with lower capacity.

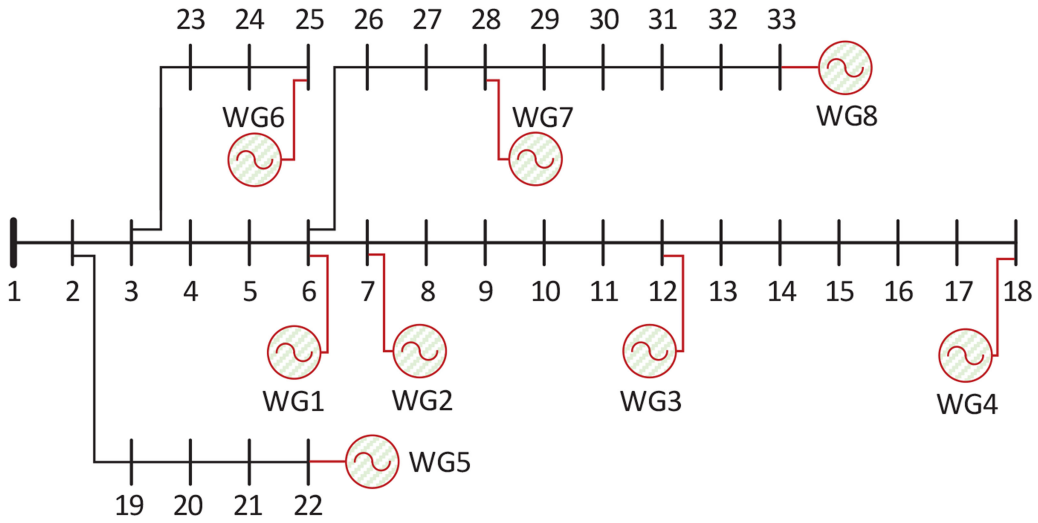

Fig. 2 *One-line diagram of the modified 33-bus radial distribution grid*

Table 5 Results of implementing BAU operation of WGs and two smart grid control strategies

Index	BAU			CVC			PFc	
	0.98lag	Unity	0.98lead	0.98lag	Unity	0.98lead	No CVC	CVC
MOI	0.2225	0.2061	0.1737	0.2747	0.2412	0.2015	0.2965	0.3449
LI	0.6467	0.6797	0.7436	0.5814	0.6462	0.7212	0.5090	0.4484
VI	1.0918	1.0919	1.0910	1.1308	1.1285	1.1241	1.1020	1.1382
Min V, p.u.	0.9515	0.9515	0.9515	0.9679	0.9679	0.9679	0.9605	0.9799
WG size, MW	3.0700	3.2410	3.2010	4.0900	3.8240	3.2530	3.5020	4.2540

CVC: coordinated voltage control and PFc: adaptive power factor control.

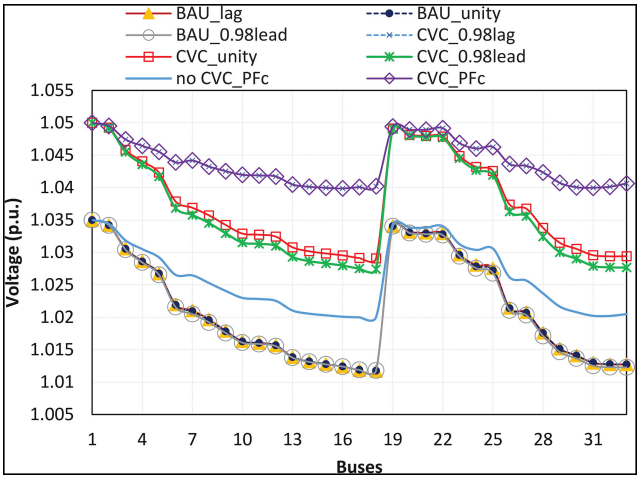

Fig. 3 *Voltage profile in the extreme state 10, i.e. maximum WG output at the minimum load level*

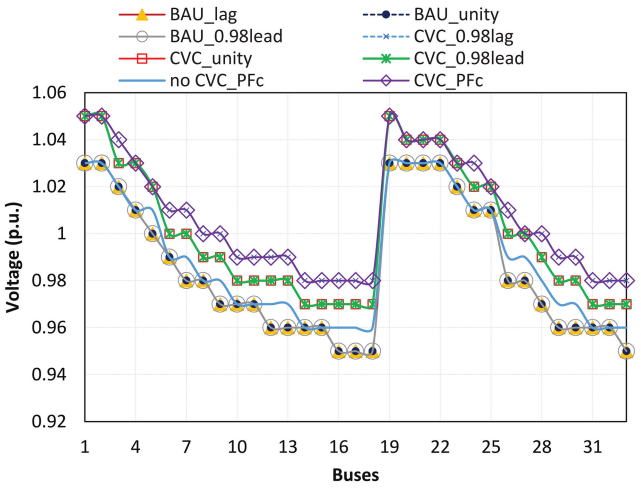

Fig. 4 *Voltage profile in the extreme state 111, i.e. minimum WG output at the maximum load level*

According to the notion of the proposed stochastic-convex OPF method, the WG capacity allocation under any operating conditions will not jeopardise the security of the DS. For example, the voltage profile on the main feeder buses during the worst states is still within the acceptable limits as shown in Figs. 3, 4 and Table 5. Generally speaking, the worst states usually correspond to the maximum WG output at the minimum load level (state 10, see Table 3), and no WG output at the maximum load level (state 111 in Table 3).

Optimal capacity of WGs at each candidate bus considering different operating scenarios is shown in Fig. 5. As seen, the largest nominal capacities are allocated closer to the load centre, i.e. bus 25. Also, buses 7, 33, and 28, are allowed to be installed large nominal capacities. The lowest WG capacity is located near to the substation nodes, i.e. buses 22 and 18.

5 Conclusion

This paper introduced a convex probabilistic planning technique for optimal allocation of wind-based DGs in DSs to maximise the multiobjective performance index including energy losses reduction and voltage improvement impact indices. The results demonstrated that the uncertainties of both demand and generation are needed to be taken into account in order to avoid over or underestimating the benefits of DG integration. Therefore, the proposed technique can closely mimic the actual technical impact calculations resulting in more accurate figures compared to those techniques based on examining scenarios where demand and generation are considered to be static. Also, the results indicated that the proposed stochastic convex OPF technique based on SOCP relaxation guarantees the optimum allocation of the wind-based DG units for all possible operating conditions which will provide a useful database for the system operator. It is observed that the voltage profile on the main feeder buses during the extreme states is still within the acceptable limits. In addition, the objectives of energy losses minimisation and voltage profile maximisation tend to compromise the potential renewable generation capacity that could be installed within distribution networks. The optimisation problem has demonstrated that adopting smart grid-based control schemes such as CVC and PFc can harvest significant benefits in

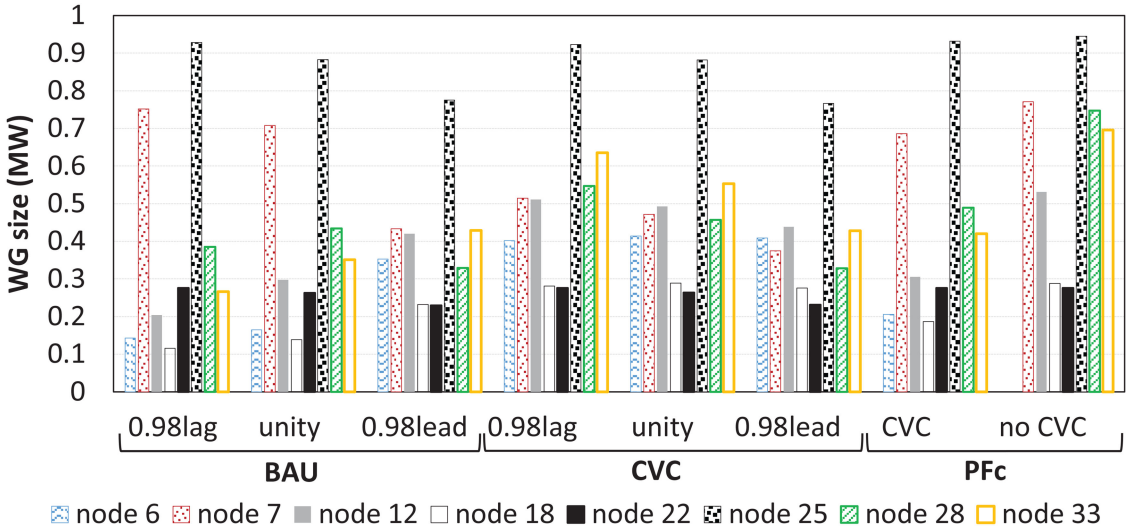

Fig. 5 *Optimal size of WG at each candidate bus considering BAU operation and two different smart grid strategies*

terms of loss reduction and voltage improvement. Since the mathematical formulation is generic, the objective function can be expanded to augment additional performance metrics such as reliability, economic and environmental concerns of DGs integration, and therefore this technique has different applications in addition to the minimisation of energy losses and voltage profile maximisation. Thus, this less complex planning problem could be easily implemented in most operation and planning practices in distribution networks.

6 References

[1] Renewables 2015 Global Status Report. Available at http:www.ren21.net/

[2] Masson, M.L.G., Biancardi, D.: 'Global market outlook for photovoltaics until 2016'. Available at http://www.epia.org/news/

[3] Quezada, V.H.M., Abbad, J.R., Roman, T.G.S.: 'Assessment of energy distribution losses for increasing penetration of distributed generation', *IEEE Trans. Power Syst.*, 2006, **21**, (2), pp. 533–540

[4] Shayani, R.A., de Oliveira, M.A.G.: 'Photovoltaic generation penetration limits in radial distribution systems', *IEEE Trans. Power Syst.*, 2011, **26**, (3), pp. 1625–1631

[5] Ochoa, L.F., Padilha-Feltrin, A., Harrison, G.P.: 'Evaluating distributed time-varying generation through a multiobjective index', *IEEE Trans. Power Deliv.*, 2008, **23**, (2), pp. 1132–1138

[6] Akbari, M.A., Aghaei, J., Barani, M., *et al.*: 'New metrics for evaluating technical benefits and risks of DGs increasing penetration', *IEEE Trans. Smart Grid*, 2017, (9) early access

[7] Aghaei, J., Akbari, M., Roosta, A., *et al.*: 'Integrated renewable conventional generation expansion planning using multiobjective framework', *IET Gener. Transm. Distrib.*, 2012, **6**, (8), pp. 773–784

[8] Chiradeja, P., Ramakumar, R.: 'An approach to quantify the technical benefits of distributed generation', *IEEE Trans. Energy Convers.*, 2004, **19**, (4), pp. 764–773. doi: 10.1109/TEC.2004.827704

[9] Lee, S.-H., Park, J.-W.: 'Selection of optimal location and size of multiple distributed generations by using Kalman filter algorithm', *IEEE Trans. Power Syst.*, 2009, **24**, (3), pp. 1393–1400

[10] Hung, D.Q., Mithulananthan, N.: 'Multiple distributed generator placement in primary distribution networks for loss reduction', *IEEE Trans. Ind. Electron.*, 2013, **60**, (4), pp. 1700–1708

[11] Hung, D.Q., Mithulananthan, N., Lee, K.Y.: 'Determining PV penetration for distribution systems with time-varying load models', *IEEE Trans. Power Syst.*, 2014, **29**, (6), pp. 3048–3057

[12] Vatani, M., Alkaran, D.S., Sanjari, M.J., *et al.*: 'Multiple distributed generation units allocation in distribution network for loss reduction based on a combination of analytical and genetic algorithm methods', *IET Gener. Transm. Distrib.*, 2016, **10**, (1), pp. 66–72

[13] Liew, S.N., Strbac, G.: 'Maximising penetration of wind generation in existing distribution networks', *IEE Proc., Gene. Transm. Distrib.*, 2002, **149**, (3), pp. 256–262

[14] Atwa, Y., El-Saadany, E., Salama, M., *et al.*: 'Optimal renewable resources mix for distribution system energy loss minimization', *IEEE Trans. Power Syst.*, 2010, **25**, (1), pp. 360–370

[15] Koutroumpezis, G., Safigianni, A.: 'Optimum allocation of the maximum possible distributed generation penetration in a distribution network', *Electr. Power Syst. Res.*, 2010, **80**, (12), pp. 1421–1427

[16] Atwa, Y.M., El-Saadany, E.F.: 'Probabilistic approach for optimal allocation of wind-based distributed generation in distribution systems', *IET Renew. Power Gener.*, 2011, **5**, (1), pp. 79–88

[17] Al Abri, R., El-Saadany, E.F., Atwa, Y.M.: 'Optimal placement and sizing method to improve the voltage stability margin in a distribution system using distributed generation', *IEEE Trans. Power Syst.*, 2013, **28**, (1), pp. 326–334

[18] Kim, K.-H., Song, K.-B., Joo, S.-K., *et al.*: 'Multiobjective distributed generation placement using fuzzy goal programming with genetic algorithm', *Eur. Trans. Electr. Power*, 2008, **18**, (3), pp. 217–230

[19] El-Ela, A.A., Allam, S.M., Shatla, M.: 'Maximal optimal benefits of distributed generation using genetic algorithms', *Electr. Power Syst. Res.*, 2010, **80**, (7), pp. 869–877

[20] Pandi, V.R., Zeineldin, H., Xiao, W.: 'Determining optimal location and size of distributed generation resources considering harmonic and protection coordination limits', *IEEE Trans. Power Syst.*, 2013, **28**, (2), pp. 1245–1254

[21] Abu-Mouti, F.S., El-Hawary, M.: 'Optimal distributed generation allocation and sizing in distribution systems via artificial bee colony algorithm', *IEEE Trans. Power Deliv.*, 2011, **26**, (4), pp. 2090–2101

[22] Rao, R.S., Ravindra, K., Satish, K., *et al.*: 'Power loss minimization in distribution system using network reconfiguration in the presence of distributed generation', *IEEE Trans. Power Syst.*, 2013, **28**, (1), pp. 317–325

[23] Banerjee, B., Islam, S.M.: 'Reliability based optimum location of distributed generation', *Int. J. Electr. Power Energy Syst.*, 2011, **33**, (8), pp. 1470–1478

[24] Lobo, S.B.M.S., Vandenberghe, L., Lebret, H.: 'Applications of second-order cone programming', *Linear Algebr. Appl.*, 1998, **284**, pp. 193–228

[25] Shezan, S., Das, N., Mahmudul, H.: 'Techno-economic analysis of a smart-grid hybrid renewable energy system for Brisbane of Australia', *Energy Procedia*, 2017, **110**, pp. 340–345

[26] Jayaweera, D., Islam, S., Neduvelil, S.: 'Two-stage approach for the assessment of distributed generation capacity mixture in active distribution networks', *J. Renew. Sustain. Energy*, 2013, **5**, (5), p. 053120

[27] Pinheiro, J.M.S., Dornellas, C.R.R., Schilling, M.T., *et al.*: 'Probing the new IEEE reliability test system (RTS-96): HL-II assessment', *IEEE Trans. Power Syst.*, 1998, **13**, (1), pp. 171–176

[28] Singh, C., Kim, Y.: 'An efficient technique for reliability analysis of power systems including time dependent sources', *IEEE Trans. Power Syst.*, 1988, **3**, (3), pp. 1090–1096

[29] Boyle, G.: '*Renewable energy*' (Oxford University Press, 2004)

[30] Baran, M.E., Wu, F.F.: 'Network reconfiguration in distribution systems for loss reduction and load balancing', *IEEE Trans. Power Deliv.*, 1989, **4**, (2), pp. 1401–1407

[31] Capitanescu, F., Ochoa, L.F., Margossian, H., *et al.*: 'Assessing the potential of network reconfiguration to improve distributed generation hosting capacity in active distribution systems', *IEEE Trans. Power Syst.*, 2015, **30**, (1), pp. 346–356

[32] McCarl, B.A., Meeraus, A., van der Eijk, P., *et al.*: 'McCarl GAMS user guide', 2014. Available at http://www.gams.com

[33] Wang, S., Chen, S., Ge, L., *et al.*: 'Distributed generation hosting capacity evaluation for distribution systems considering the robust optimal operation of OLTC and SVC', *IEEE Trans. Sustain. Energy*, 2016, **7**, (3), pp. 1111–1123